Accurate absolute measurement of trapped Cs atoms in a MOT

M. Talavera O.[a,b], M. López R.[a], E. de Carlos L.[a], and S. Jiménez S.[b]
[a] *División de Tiempo y Frecuencia, Centro Nacional de Metrología, CENAM, km 4.5 Carretera a los Cués, El Marques, Querétaro, 76241, México.*
[b] *Centro de Investigación y Estudios Avanzados del IPN, Unidad Querétaro, Libramiento Norponiente No. 2000, Fracc. Real de Juriquilla, Qro, 76230 México.*

Recibido el 16 de enero de 2007; aceptado el 28 de junio de 2007

A Cs-133 Magneto-Optical Trap (MOT) has been developed at the Time and Frequency Division of the Centro Nacional de Metrología, CENAM, in Mexico. This MOT is part of a primary frequency standard based on ultra-cold Cs atoms, called CsF-1 clock, under development at CENAM. In this Cs MOT, we use the standard configuration ($\sigma^+ - \sigma^-$) 4-horizontal 2-vertical laser beams 1.9 cm in diameter, with 5 mW each. We use a 852 nm, 5 mW, DBR laser as a master laser which is stabilized by saturation spectroscopy. Emission linewidth of the master laser is 1 MHz. In order to amplify the light of the master laser, a 50 mW, 852 nm AlGaAs laser is used as slave laser. This slave laser is stabilized by light injection technique. A 12 MHz red shift of the light is performed by two double passes through two Acusto-Optic Modulators (AOMs). The optical part of the CENAMs MOT is very robust against mechanical vibration, acoustic noise and temperature changes in our laboratory, because none of our diode lasers use an extended cavity to reduce the linewidth. In this paper, we report results of our MOT characterization as a function of several operation parameters such as the intensity of laser beams, the laser beam diameter, the red shift of light, and the gradient of the magnetic field. We also report accurate absolute measurement of the number of Cs atoms trapped in our Cs MOT. We found up to 6×10^7 Cs atoms trapped in our MOT measured with an uncertainty no greater than 6.4%.

Keywords: Time and Frequency Metrology; cold Cs atoms; MOT; diode lasers; laser stabilization.

Una Trampa Magneto-Óptica (MOT) de Cs-133 se ha desarrollado en la División de Tiempo y Frecuencia del Centro Nacional de Metrología, CENAM, en México. Esta MOT es parte de un patrón primario de frecuencia basado en átomos ultra fríos de Cs, llamado reloj CsF-1 que se encuentra en desarrollo en el CENAM. En esta MOT de Cs, se emplea la configuración estándar ($\sigma^+ - \sigma^-$) de 4 haces láser horizontales y 2 verticales de 1.9 cm de diámetro con 5 mW de potencia cada uno. Se utiliza un láser DBR de 852 nm y 5 mW como láser maestro estabilizado por espectroscopia de saturación. El ancho de línea de emisión del láser maestro es de 1 MHz. Para amplificar la luz del láser maestro, se emplea un láser esclavo de AlGaAs de 852 nm y 50 mW de potencia. Este láser esclavo es estabilizado por la técnica de inyección de luz. Se realiza un corrimiento de la luz al rojo de 12 MHz por un doble paso a través de dos Moduladores Acusto-Ópticos (AOMs). La parte óptica de la MOT del CENAM es muy robusta contra la vibración mecánica, el ruido acústico y los cambios de temperatura en el laboratorio, debido a que ninguno de los diodos láser emplea una cavidad extendida para reducir el ancho de línea. En este trabajo se reportan los resultados de la caracterización de la MOT como una función de varios parámetros de operación tales como: intensidad y diámetro de los haces láser, corrimiento al rojo de la luz y el gradiente de campo magnético. También se reportan mediciones absolutas del número de átomos de Cs atrapados en la MOT. Se encontraron más de 6×10^7 átomos de Cs atrapados, medidos con una incertidumbre que en ningún caso es mayor a 6.4%.

Descriptores: Metrología de Tiempo y Frecuencia; átomos de Cs fríos; MOT; láseres diodo; estabilización láser.

PACS: 32.80.Pj; 42.62.Eh; 06.30.Ft

1. Introduction

Trapping and cooling atoms in a magneto-optical trap (MOT) constitutes a very valuable technique in the study of different aspects of fundamental physics [1]. Ultra cold atoms also have important applications when measuring time with the highest accuracy [2]. For example, the so called *fountain clocks* use a Magneto-Optical Trap (MOT), where the number of trapped Cs-133 atoms is one of the most important parameters in the uncertainty of the experimental reproduction of the unit of time, the second [3]. In the high accuracy time measurement applications, there is a compromise between the number of trapped atoms and the frequency stability and accuracy of the clock. The frequency stability $\sigma_y(\tau)$ is related to the signal-to-noise ratio S/N of the Ramsey pattern around the so-called *clock transition* according to the relation [2]

$$\sigma_y(\tau) = \frac{1}{S/N}\frac{1}{\nu/\Gamma}\tau^{1/2} \tag{1}$$

where ν is the central frequency of the quantum transition, Γ is the FWHM transition linewidth and τ is an integration time. On the other hand, it is well known that the signal-to-noise ratio is proportional to the number of atoms trapped in the MOT. However, the uncertainty in the evaluation of the frequency shift due to collisions among Cs atoms increases as a function of the density of the atoms. Accurate measurement of the number of Cs atoms trapped in a MOT is important when evaluating the uncertainty of the experimental realization of the unit of time, the second. Accurate counting of trapped Cs atoms could also have interesting applications in mass measurement. The unit of mass of the International Systems of Units (SI) is currently defined in terms of the mass of one particular artifact, a cylinder made of a platinum and

iridium mixture [4]. However, the *Bureau International des Poids et Measures* (BIPM) has recommended to the international scientific community [5] the development of experiments toward a redefinition of the kilogram in terms of fundamental constants. So far, different techniques have been developed that lead towards a new definition of the kilogram of the SI in terms of the Planck constant through the Watt balance [6], the Avogadro's constant through the so-called Silicon sphere [7], or the mass of gold atoms by capturing gold atoms in a atomic beam experiments [8]. Accurate measurement of the absolute number the Cs atoms trapped in a MOT could also have applications in mass measurements using the mass of the Cs atom as a point of reference.

Some technical publications report the number of atoms trapped in a MOT [9], however none presents a report that aims at measuring the absolute large number ($> 10^6$) of trapped Cs atoms with the highest possible accuracy. The main goal of this work is to report our results of measurements of the absolute number of Cs atoms trapped in a MOT with high accuracy. We include, of course, an exhaustive uncertainty analysis in our measurements.

In Sec. 2, we describe the experimental setup of the MOT used to accurately measure the number of trapped Cs atoms. In Sec. 3 we present experimental results showing the dependence of trapped atoms as a function of different parameters including: intensity of the laser beams, red frequency shift, diameter of the laser beams and magnetic field gradient. A discussion of the experimental results is presented in Sec. 4, making an uncertainty analysis of our measurements. Finally, the conclusions of this work are presented in Sec. 5.

2. Experimental setup

Mechanisms for cooling and trapping neutral atoms in a MOT have been extensively explained in different articles [10] and special issues [11]. We will not reproduce those well known mechanisms in this paper. A theoretical approach to the capture and loss process of the atoms in the MOT can be found in Refs. 12 to 14. Instead, we shall focus on the relevant experimental parts needed to measure with high accuracy the number of atoms trapped in a Cs MOT.

The Cs MOT developed at CENAM consists of a sphere made stainless steel about 15 cm in diameter and with 12 optical ports. Six of the 12 optical ports are used to feed the sphere with the cooling and repumping lasers beams. In each of those six ports there is an coated, optical antireflection window for 852 nm (transmission coefficient better than 99%). Figure 1 shows the stainless steel sphere with the optical port. The vacuum in the sphere, without Cs, is around 10^{-8} Pa. Partial Cs pressure is maintained around 10^{-6} Pa, and it is controlled through the temperature of the Cs reservoir and a valve. The sphere is surrounded by two coils, each of them 20 cm in diameter, arranged in an anti-Helmholtz configuration. The magnetic field gradient close to the center of the sphere is 5 G/cm; it can be changed by adjusting the current through the coils. Electric current in the anti-Helmholtz coils is typically 2 Å. The light of the MOTs optical system is produced by three diode lasers, the master, the slave and the repumping lasers. The master laser consists of a DBR type diode laser manufactured by Yokowaga (model YL85XTW), with 5 mW output power, 1 MHz in linewidth, and 852 nm in wavelength. In Ref. 15, there are reports of the use of DBR lasers in Cs atomic clocks, and in Ref. 16 in Rb clocks. The master DBR laser is stabilized at the $\left|6^2 s_{1/2}, F=4\right\rangle \rightarrow \left|6^2 p_{3/2}, F'=5\right\rangle$ transition using the modulated frequency spectroscopy technique [17]. Figure 2 shows the measurement results on the typical frequency stability of three DBR lasers using the "three-cornered hat method" [18].

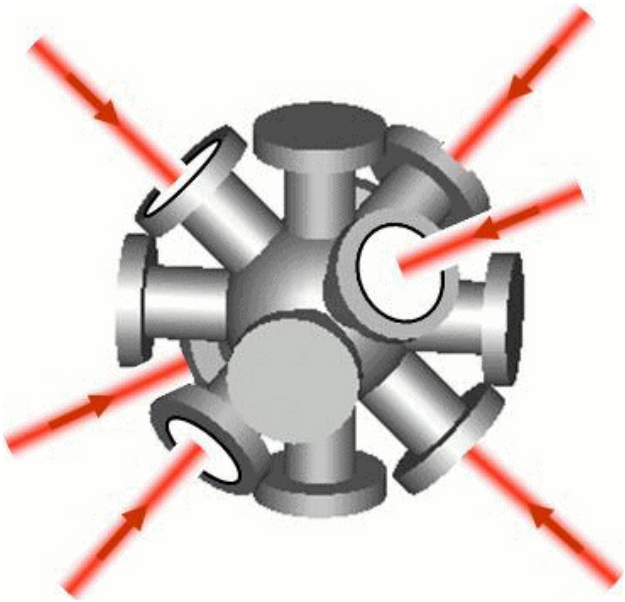

FIGURE 1. Sphere of stainless steel with 12 optical ports, six of the 12 optical ports have an antireflection coated optical window for 852 nm (transmission coefficient better than 99%), and they are used to feed the sphere with the cooling and repumping laser beams.

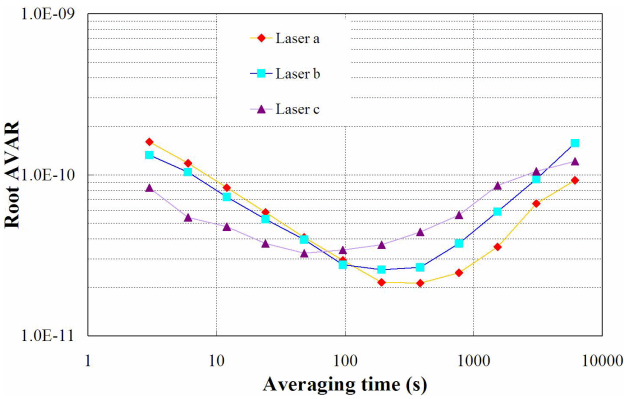

FIGURE 2. Estimation of the absolute frequency stability of three DBR lasers stabilized to the D_2 line of Cs-133 (852 nm) using the "three-cornered hat method" [18].

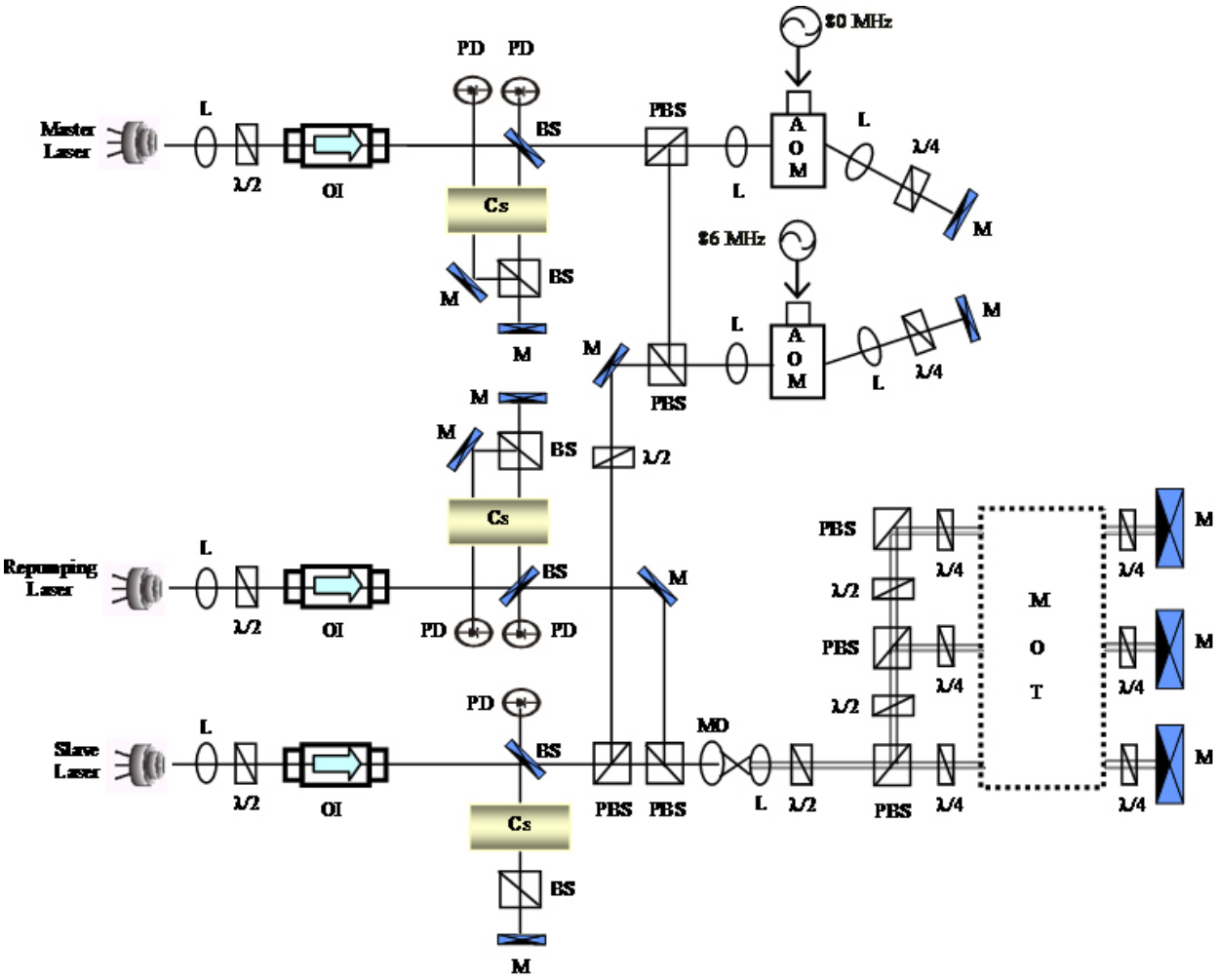

FIGURE 3. Schematic diagram of configuration of CENAMs MOT. Here M is for mirror, $\lambda/4$ is for $1/4$ wave plate, $\lambda/2$ represents a $1/2$ wave plate, BS stands for beam splitter, PBS is for polarized beam splitter, AOM is an acousto-optic modulator, L represents a lens, IO is an optical isolator, MO represents a microscope objective and PD represents a photodetector.

Two Acousto-optic Modulators, AOMs, are used to shift the light to the red around 12 MHz. Two double passes of light through the AOMs combined with the cat's eye configuration are used to shift the frequency of the laser light. The slave laser was manufactured by Blue Sky Research, model VPLS-0852-050-X-9-C, output power 50 mW, 852 nm in wavelength. It has a single spatial Gaussian mode for far field. So, a circular cross-section light beam output is obtained with a relationship of circularity of 1.2:1.0, resulting in a highly homogeneous intensity distribution. This characteristic emission of the slave laser avoids the need to use a pinhole as spatial filter, giving us the opportunity to feed into the MOT, in a very efficient way, a large part of its output power. The slave laser is stabilized by the injection light technique [19,20] feeding about 200 μW of light from the master laser after the red frequency shift. Then the circular laser beam is directed through a lens system in order to expand it to 4 cm in diameter (this diameter is defined by the $1/e^2$relation). With the help of a diaphragm, the final diameter of the cooling beam fed into the sphere is controlled. It is important to mention that even at the smallest diameter (≈ 0.7 cm), diffraction effects from the diaphragm were found to be negligible. After that, the cooling beam is divided into three beams of around 5 mW of power each, and then fed into the MOT. Due to the small emission linewidth of the master laser, neither the master nor the slave laser are under the extended cavity configuration. The repumping laser is similar to the master laser (same manufacturer and model), but it is stabilized to the $\left|6^2 s_{1/2}, F=3\right\rangle \rightarrow \left|6^2 p_{3/2}, F'=4\right\rangle$ Cs transition by saturation spectroscopy. Light from the repumping laser is superimposed on the six cooling beams. A $1/4$-wave plate is used in each window of the sphere in order to have $\sigma^+ - \sigma^-$ polarizations. The standard geometrical arrangement of the cooling lasers is used, with four laser beams on the horizontal plane and two laser beams in the vertical direction. Due to the absence of an extended cavity in the lasers, the CENAMs MOT is highly insensitive to acoustic noise and temperature changes in the laboratory. The MOT is routinely operated and no major adjusting is needed between daily operation sessions. However, it is necessary to mention that we found that

our DBR lasers are highly sensitive to noise (harmonics and other frequencies) in the AC plug power supply. In order to avoid this inconvenience, we normally use a set of DC batteries to operate our MOT. Figure 3 shows schematically the optical system of the CENAMs MOT.

3. Experimental results

As we mentioned previously, the results shown in this paper are part of the measurements taken in order to determine accurately the number of atoms trapped in our MOT as a function of several parameters, including: intensity, diameter of cross section, red shift of the laser beams and magnetic field gradient. The number of trapped Cs atoms has been estimated by measuring the fluorescence of the cloud of trapped atoms while it is illuminated with the cooling and repumping beams.

If r is the rate of photons scattered by a single Cs atom while it is illuminated with the cooling beams, then $rh\nu$ is the emitted power carried by one atom due to the spontaneous decay. Here h is the Planck constant and ν is the central frequency corresponding to the cyclic $\left|6^2s_{1/2}, F=4\right\rangle \rightarrow \left|6^2p_{3/2}, F'=5\right\rangle$ Cs transition. If N is the number of atoms trapped in the MOT under the steady-state condition [14], then $Nrh\nu$ is the power carried by the fluorescence photons. Finally, the power detected by a photodetector due to fluorescence of the trapped atoms in the MOT can be written as:

$$P = \Omega N r h\nu, \tag{2}$$

where Ω is the solid angle defined by the photodetector with respect to the cloud of trapped Cs atoms. Solving for the number of trapped atoms in terms of power measurement, and assuming that all atoms in the trap scatter photons at some average rate, we have $N = P/\Omega r h\nu$. In Eq. (2) we are modeling the cloud of trapped atoms as a point source. The rate of photons scattered by a single atom can be expressed as [21]:

$$r = \frac{1}{2/\Gamma}\frac{C^2\varsigma}{(1+C^2\varsigma)}, \tag{3}$$

where

$$\varsigma = \frac{I/I_s}{1+(2\Delta\Gamma)^2}, \tag{4}$$

Here I is the intensity of the laser beams, $I_s = 1.102$ mW/cm^2 is the Cs saturation intensity [21] for the case of the $\left|6^2s_{1/2}, F=4, m_F=4\right\rangle \rightarrow \left|6^2p_{3/2}, F'=5, m_F=5\right\rangle$ cyclic transition, Δ is the frequency shift of the laser beams with respect to the atomic frequency transition, $\Gamma = 5.3$ MHz is the FWHM linewidth of the cooling transition. C is a phenomenological factor which is introduced in order to take into account the effect of the reduced saturation. C is related to the average of the Clebsch-Gordan coefficients for the different possible transitions between various magnetic sublevels for the atoms in the MOT [22]. For the $\left|6^2s_{1/2}, F=4\right\rangle \rightarrow \left|6^2p_{3/2}, F'=5\right\rangle$ transition, the average of the squares of the Clebsch-Gordan coefficients is $0.4 < C^2 < 1$ [22]. The experimental value considered in this paper is $C = 0.7 \pm 0.2$ [21], indicating a preferential population on the high m_F stretched states.

To determine the absolute number of trapped atoms from the emitted fluorescence, according to (2), a photodetector can be used to measure a fraction of the total fluorescence emitted by the atoms trapped in the MOT. When using this method, it is important to collect into the photodetector as much fluorescence as possible. In this experiment, measurements taken from the photodetector made the biggest contribution in the uncertainty analysis, as is shown in Sec. 4. Careful attention was paid to the different parameters involved in this power measurement as needed to ensure high accuracy in the N measurement. So, from accurate power measurements we determine the number of trapped atoms. In order to carry out the accurate optical power measurements of the fluorescence in our MOT, we use a measurement system which includes a photodetector, a trans-impedance amplifier and a multimeter. The entire system was calibrated using high accurate a power optical standard. The value of the radiant sensitivity S of the photodetector (Hamamatsu S1337 1010BQ) obtained by the calibration process was 0.4574 A/W at $\lambda = 852$nm, with an uncertainty no larger than 2%. This uncertainty value takes into account variations of the radiant sensitivity across the photodetectors sensitive surface (1 cm^2). Figure 4 shows a cross section of the stainless steel sphere in our MOT, where it is indicating the photodetectors position.

Between the trapped Cs atoms and the photodetector, there is no optical element except for the optical window. The optical window has an antireflection coat on both sides for 852 nm. The transmission coefficient of the windows is high, better than 0.9987. In our experiments, we have carefully

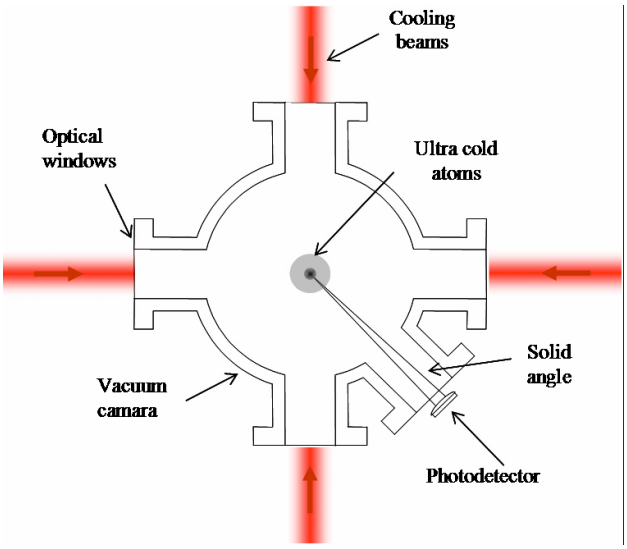

FIGURE 4. Lateral view of our MOT, indicating the photodetector position.

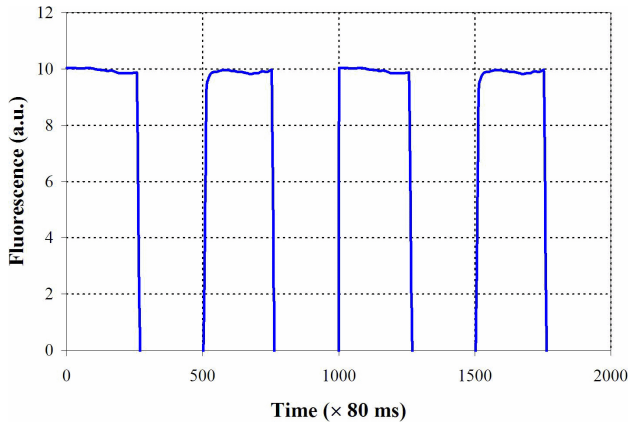

FIGURE 5. Intensity of light in the Cs MOT's photodetector as a function of time while the trap is loaded and unloaded by turning off the cooling beams. The MOT parameters are Δ= -10 MHz, I= 1.5 mW/cm^2, d= 1.9 cm and ∇B=5.3 G/cm.

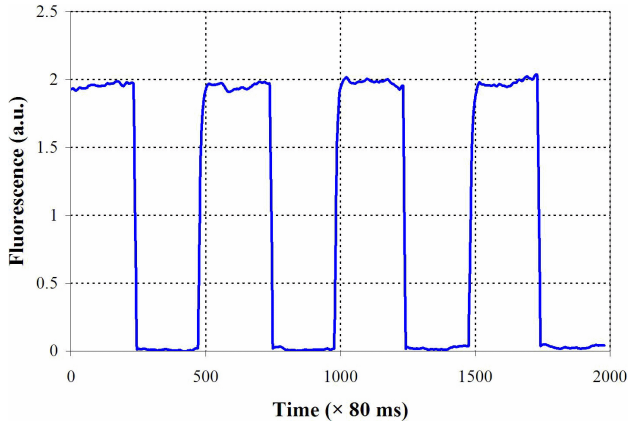

FIGURE 6. Signal on the photodetector resulting from the florescence of the trapped Cs atoms. The MOT parameters are Δ= -10 MHz, I= 1.5 mW/cm^2, d= 1.9 cm and ∇B=5.3 G/cm.

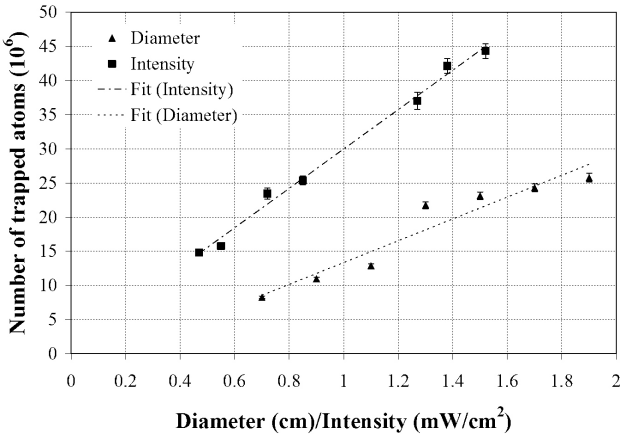

FIGURE 7. Measurements of the number of trapped Cs atoms in the CENAMs MOT as a function of the intensity and diameter of the cooling beams. ∇B = 5.3 G/cm and Δ= -12 MHz.

verified the linearity in our optical power measurement system in order to avoid any electronic saturation effect.

In order to set the photodetectors sensitive surface in a parallel position with respect to the optical window, the photodetector was mounted on a customized mechanical device which includes a translation system. Three micrometer screws facilitate the 3-dimensional tilting motion of the photodetector. With this mechanical system we provide a convenient method of alignment of the photodiode. The best signal-to-noise ratio is obtained when the photodetector surface is placed parallel to the optical window. In order to avoid detection of light coming from the laboratory environment, a mask is used in the view-port, carefully fitted to the sensitive surface of the photodetector. We also designed an enclosure to cover the MOT, completely in order to minimize the light feeding from the laboratory environment. In all cases, measurements were carried out when the environmental light in the laboratory was turned off.

On the other hand, measurements of the diameter of the cold Cs atoms in the MOT were made in a simple way through a CCD camera (Mega Speed, CPL MS-4K model) sensitive to 852 nm. The image size of the cloud of cold Cs atoms produced by the CCD camera was compared to the image size of the opposite window on the stainless steel sphere also appearing in the CCD image. The diameter was 4 mm $\pm$ 0.2 mm.

Figure 5 shows the intensity of light on the photodetector as a function of time while the trap is loaded and unloaded by turning off the cooling beams. The signal increases to a saturation level with a time constant $\tau \approx 1$ s. Then, the cooling laser beams and the magnetic field gradient were held constant for around 20 seconds; after that time the laser beams were switched off and the signal returned to zero. It is important to keep the mind that the measurements of the intensity of light shown in Fig. 5 are the result of the fluorescence from the cloud of cooled Cs atoms and the straight light of the cooling beams by the walls and windows of the vacuum container during the measurement time, as well as the fluorescence light from non trapped Cs atoms (fluorescence from the path of cooling beams). In order to get the contribution of the photodetector of light coming from the cooled Cs atoms, we subtract from the measurements shown in Fig. 5 the signal obtained when the magnetic field gradient is turned off, that is, the cooling lasers beams are on but there are no trapped Cs atoms. During those measurements, care was taken to avoid any contribution from other sources of light (like laboratory environmental light for example). In Fig. 6 we show the signal on the photodetector resulting from the florescence of the Cs trapped atoms.

Figures 7-9 show the dependence of the number of Cs atoms trapped in the MOT as function of several operation parameters. The cooling laser beams were carefully aligned to obtain spherical cloud shapes. Figure 7 shows the number of the trapped Cs atoms as a function of the intensity and diameter of the cooling laser beams. In that graph, while we changed the trapping beam intensities by placing neutral

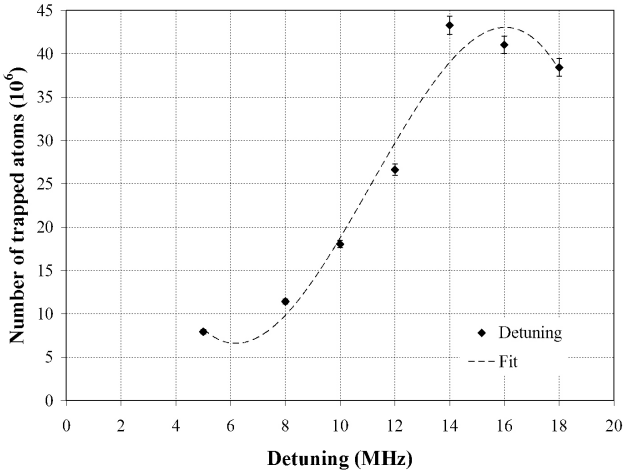

FIGURE 8. Number of trapped Cs atoms in the CENAMs MOT as a function of laser detuning, with a diameter of laser cooling beams of 1.9 cm, intensity of cooling beams of 1.5 mW/cm^2, and ∇B= 5.3 G/cm.

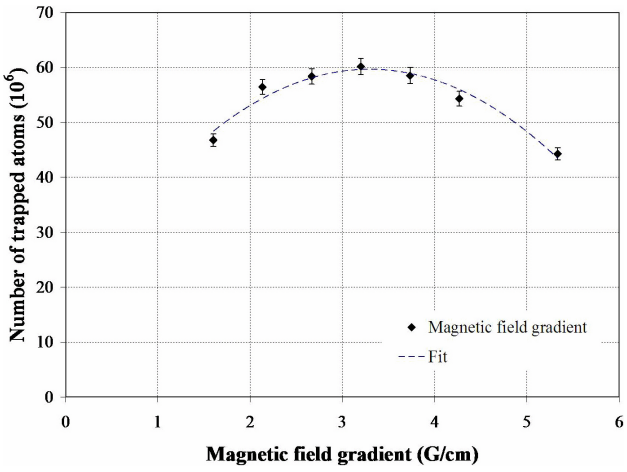

FIGURE 9. Number of trapped Cs atoms in the CENAMs MOT as a function of the magnetic field gradient. Diameter of the cooling laser beams was 1.9 cm, laser detuning 14 MHz, and intensity of cooling beams 1.5 mW/cm^2.

density filters in the beam path before it is split into three parts, the diameter was kept constant at 1.9 cm. On the other hand, while we changed the diameter by placing a diaphragm, the intensity of the cooling laser beams was kept constant at 1.5 mW/cm^2. In all these measurements, the magnetic field gradient remains constant at 5.3 G/cm.

As can be noticed from these graphs, our results show that the number of trapped Cs atoms has a linear dependence on the intensity and diameter of the cooling beams.

Figure 8 shows how the number of trapped Cs atoms depends on the detuning of the cooling lasers beams while the magnetic field gradient remains constant, as well as the intensity and diameter of the laser beams. Laser detuning was changed by adjusting the frequency of the AOMs. As can be seen in Fig. 8, while the detuning of the cooling laser beams increased for a given beam intensity and diameter, the number of atoms increases to reach an optimum value and after that it decays. These results are in close agreement with those in Ref. 12. However, the results in Ref. 12 do not include uncertainty values.

Figure 9 shows how the number of trapped atoms depends on the magnetic field gradient at a fixed detuning, diameter and intensity of cooling laser beams. The magnetic field gradient was changed by adjusting the current in the anti-Helmholtz coils. The magnetic field gradient changes both the loading time constant and the number of trapped Cs atoms in the steady state condition. We observe that when the diameter of the cooling beams was 1.9 cm, the small magnetic field gradient causes an increase in the loss rate due to collisions of the trapped Cs atoms with non-trapped atoms. On the other hand, when the magnetic field gradient increases to 5.3 G/cm, the capture rate diminishes, resulting in a smaller number of trapped Cs atoms.

In our experiment, the optimum values for the MOT's parameters in order to trap the largest number of Cs atoms are: 3.2 G/cm for the magnetic field gradient, 1.9 cm for the diameter and 1.5 mW/cm^2 for the intensity of cooling laser beams along with a laser detuning of 14 MHz. These results are in agreement (for the overlap region), within uncertainties, with those previously published by K. Lindquist, M Stephens, and C. Wieman in Ref. 23.

4. Uncertainty analysis

The uncertainty μ_N associated with the measurement of the number of trapped Cs atoms is presented in this section. This analysis is based on the *Guide to the Expression of Uncertainty in Measurement* (GUM) [24]. According to the mathematical model presented in a previous section, the number $N$of trapped Cs atoms in the MOT is a function of the optical power P of fluorescence from the cold atoms, the solid angle Ω of the photodetector with respect to the cloud of Cs cold atoms, the rate of photons scattered r for the cycling transition and the energy of the fluorescence photons $h\nu$. So we can write that $N = N\,(P, \Omega, r, \nu)$. Thus, in according to the GUM, the uncertainty μ_N in the number of trapped Cs atoms in our MOT can be written as follows:

$$\mu_N = \sqrt{\left[\left(\frac{\partial N}{\partial P}\right)\cdot\mu_P\right]^2 + \left[\left(\frac{\partial N}{\partial \Omega}\right)\cdot\mu_\Omega\right]^2 + \left[\left(\frac{\partial N}{\partial r}\right)\cdot\mu_r\right]^2 + \left[\left(\frac{\partial N}{\partial \nu}\right)\cdot\mu_\nu\right]^2} \tag{5}$$

where μ_P is the uncertainty associated with power measurements of the fluorescence in our MOT. This includes the uncertainty associated with the whole optical power measurement system, the uncertainty for repeatability and the uncertainty for reproducibility; μ_Ω is the uncertainty associated with the solid angle, μ_r is the uncertainty associated with the scattering rate of photons, and μ_ν is the uncertainty associated to laser frequency. The ability to vary just one trap parameter while holding the others constant offers a convenient method for systematically measuring the number of trapped atoms as a function of the various trap operation parameters. It is interesting to note that the most significant contribution to the uncertainty of the number of trapped Cs atoms in the MOT corresponds to the optical power measurement. Numerical values of the terms in (5) depend, of course, on the specific values for the operational parameters of the MOT. However, we can mention that the term $(\partial N/\partial P)\cdot\mu_P$ takes on values around 10^5. The next largest contribution is the uncertainty of the rate of photon dispersion $(\partial N/\partial r)\cdot\mu_r$, which is on order of magnitude smaller than that associated with the power measurements, taking on values around 10^4. In third place is the uncertainty due to the solid angle contribution $(\partial N/\partial\Omega)\cdot\mu_\Omega$, which is in the 10^3 region. Finally, with a contribution that can be ignored, the term $(\partial N/\partial\nu)\cdot\mu_\nu$ assumes values around 10^{-2}. The best uncertainty on the number of trapped Cs atoms corresponds to $N = 6\times10^7$ atoms which is $\mu_N = \pm1.4\times10^6$, less than 2.5% in N. This uncertainty is for the following values for MOT's operation parameters: intensity, diameter and red shift of cooling laser beams of 1.5 mW/cm^2, 1.9 cm and 14 MHz, respectively. In this case, the gradient of the magnetic field is 3.2 G/cm. In the worst case, which corresponds to intensity, diameter and frequency shift of the cooling laser beams of 1.5 mW/cm^2, 1.9 cm, 5 MHz, respectively, and a magnetic field gradient of 5.3 G/cm, the uncertainty in N is $\mu_N = \pm2.5\times10^5$ for $N = 7.9\times10^6$ atoms. This uncertainty value corresponds to around 3.2% of the number of trapped Cs atoms. However, in order to increase the confidence level in the uncertainty in the number of trapped Cs atoms to 95%, if we assume that values of different parameters in our MOT are Gaussian distributed, and following the recommendation of the ISO Guide to the Expression of Uncertainty in Measurements, we use a coverage factor of 2 in our uncertainty analysis to find that our uncertainty is never greater than 6.4%.

5. Conclusions

We have reported results of the characterization of a Cs MOT designed to operate a Cs fountain clock. The most significant characteristic of our Cs MOT, which is different from others MOTs, is that our optical system works with light coming from DBR diode lasers operated without extended cavities. The emission linewidth of our DBR lasers is around 1 MHz. This linewidth value is good enough to operate a Cs MOT, as we showed in this paper, and also a Cs fountain clock. Due to the absence of extended cavities in the optical system, our MOT is highly insensitive to acoustic noise and temperature changes in the laboratory. The characterization reported in this paper was made with the goal of accurate measurements of absolute number of trapped Cs atoms in our MOT as a function of several operation parameters such as the intensity of laser beams, laser beam diameter, red shift of light, and gradient of the magnetic field. Our results are in agreement with others previously reported. However our results have lower measurement uncertainties than previously published reports. We found up to 6×10^7 trapped Cs atoms in our MOT measured with an uncertainty no greater than 6.4% in all cases.

1. G. Santarelli *et al.*, *Phys. Rev. Lett* **82** (1999) 4619.
2. R. Wynands and S. Weyers, *Metrologia* **42** (2005) S64.
3. *13th Conférence Générale des Poids et Mesures* (CGPM, 1967).
4. *3rd Conférence Générale des Poids et Mesures* (CGPM, 1901).
5. B.N. Taylor, *The possible role of the fundamental constants in replacing the kilogram IEEE Trans. Instrum.Meas.* **40** (1991) 86; T.J. Quinn *Recent advances in mass standards and weighing*. *Metrology at the Frontiers of Physics and Technology* ed. L. Crovini and T.J. Quinn (Amsterdam: North-Holland 1992); M. Kochsiek and M. Gläser (ed). *Mass Metrology* (Berlin: Wiley-VCH, 2001); Z.J. Jabbour and S.L. Yaniv *The kilogram and measurements of mass and force J. Res. NIST* **106** (2000) 25; R.S. Davies *Mass metrology*. *Recent Advances in Metrology and Fundamental Constants* ed. T.J. Quinn and S. Leschiutta (Amsterdam: IOS, 2001).
6. A. Eichenberger, B. Jeckelmann and P. Richard, *Metrologia* **40** (2003) 356.
7. B.P. Kibble and I.A. Robinson, *Meas. Sci. Technol.* **14** (2003) 1243.
8. P. Becker and M. Gläser, *Meas. Sci. Technol.* **14** (2003) 1249.
9. M.–C. Gagné, J.S. Boulanger, and R.J. Douglas, *Can. J. Phys*. **76** (1998) 577.
10. J. Dalibard and C. Cohen-Tannoudji, *J. Opt. Soc. Am*. **B6** (1989) 2023.
11. H.J. Metcalf and P. van der Straten (Springer-Verlag New York, Inc. 1999).
12. C. Monroe, W. Swann, H. Robinson and C. Wieman, *Phys. Rev. Lett*. **65** (1990) 1571.
13. N. Sagna, G. Dudle, and P. Thomann, *J. Phys. B: At. Mol. Opt. Phys.* **28** (1995) 3213.
14. K. Gibble, S. Kasapi, and S. Chu, *Opt. Lett.* ***17*** (1992) 526.
15. R.E. Drullinger, D.A. Jennings, W.D. Lee, and J.M. Lopez-Romero, *Proceedings of the 1996 Conference on Precision Electromagnetic Measurements* (1996) 269.

16. J.Q. Deng *et al.*, *Proceedings of the 1997 European Frequency and Time Forum* (1997) 211.
17. E. de Carlos and J.M. López, *Rev. Mex. Fís.* **50** (2004) 569.
18. E. de Carlos and J.M. López, *Proceedings SPIE V Symposium Optics in Industry* **6046** (2005).
19. S. Kobayashi and T. Kimura, *IEEE Journal of Quantum Electronics* **QE-17** (1981) 681.
20. R.G. Hadley, *IEEE Journal of Quantum Electronics* **QE-22** (1986) 419.
21. C.G. Townsend, N.H. Edwards, C.J. Cooper, K.P. Zetie, and C.J. Foot, *Phys. Rev. A* **52** (1995) 1423.
22. J. Ashmore, *P. Thesis* (2005) 109.
23. K. Lindquist, M. Stephens, and C. Wieman, *Physical Review A* **46** (1992) 4082.
24. BIPM, IEC, IFCC, ISO, IUPAC, IUPAP, and OIML. *Guide to the Expression of Uncertainty in Measurement*, International Standards Organization, 1995.